Extracting signal via stochastic resonance in the semiconductor optical amplifier

Wulong Zhao (赵武龙), Hongjun Liu (刘红军)*, Qibing Sun (孙启兵), Nan Huang (黄 楠), Zhaolu Wang (王昭路), Jing Han (韩 靖), and Heng Sun (孙 恒)

State Key Laboratory of Transient Optics and Photonics, Xi'an Institute of Optics and Precision Mechanics, Chinademy of Sciences, Xi'an 710119, China

**Corresponding author: liuhongjun@opt.ac.cn*

Received April 15, 2016; accepted June 14, 2016; posted online July 15, 2016

The stochastic resonance based on optical bistability in the semiconductor optical amplifier is numerically investigated to extract a weak pulse signal buried in noise. The output property of optical bistability under different system parameters is analyzed, which determines the performance of the stochastic resonance. Through optimizing these parameters, the noise-hidden signal is extracted via stochastic resonance, in which the maximum cross-correlation gain higher than nine is obtained. This provides a novel technology for detecting a weak optical signal in various signal processing fields.

OCIS codes: 190.0190, 190.1450.
doi: 10.3788/COL201614.081901.

In signal detection and processing fields, noise is usually considered harmful which degrades the performance of low-level signal extraction, especially if the noise frequency is approximate with the signal. However, a weak periodic signal can be enhanced and recovered at the assistance of the appropriate intensity of noise in some certain nonlinear systems, displaying the cooperative phenomenon of the stochastic resonance[1]. Stochastic resonance has been explored in a wide scope of research fields, including electrical systems[2], biological systems[3], physics, and chemical reactions[4] since it was first verified experimentally in a Schmitt-Trigger bistable system[5]. It is not only used to interpret many natural phenomena, but it is also showing in various applications such as noisy signal detection, transmission enhancement in neurobiology[6–8], and noisy images restoration[9,10].

Early theoretical and experimental research has indicated that the conditions for stochastic resonance in a bistable system contain energetic threshold, subthreshold modulation signal, and noise source. In some optical bistable systems, stochastic resonance can be used in time domain signal processing such as noise-buried signal extraction and reconstruction[11], which can be interpreted through the particle movement in double-well potential. With a subthreshold signal and chaotic noise forcing, the particle will overcome the potential barrier and flip periodically between the double-well potential. For the field of optics, many works have been reported about stochastic resonance in the bistable dynamic systems with periodical force driving[12,13]. The research about optical bistability based upon a combination of regenerative amplification and saturation-induced refractive index change due to light injection in the semiconductor optical amplifier (SOA) have been widely reported[14–17]. However, few related works are reported about the feasibility application of extracting and enhancing optical pulse noisy signals via stochastic resonance in the SOA.

In this Letter, we report an efficient method for extracting signals obscured by the noise via stochastic resonance based on optical bistability in the SOA. The influence of system parameters, such as cavity length, mirror reflectivity, initial phase detuning, and optical antiguidance factors on bistable transmission is investigated, then the stochastic resonance is realized at a suitable bistable region by optimizing the system parameters. Its ability for processing and reconstructing the weak optical pulse signal is analyzed under different noise intensities, which is evaluated by the cross-correlation gain[18]. These results indicate that stochastic resonance in the SOA can effectively improve the detection capability of a weak optical signal.

Figure 1 illustrates the schematic diagram of the stochastic resonance generated in the SOA. A heterostructure GaAlAs/GaAs diode is used as the active medium, which is driven by a DC injection current below the threshold[19,20]. It is placed in a Fabry-Perot (F-P) cavity with cavity length L and mirror reflectivity R at each facet. The periodic pulse signal with additive noise is injected into the F-P cavity, which provides feedback for the input signal.

The response of the active medium can be described by the conventional rate equation for carrier density[15]. The phase shift across the laser diode depends on the refractive index as a variation of carrier density, and then the rate equation is converted to the differential equation for phase shift. The relationship between the input and output light intensity for the SOA can be expressed as[21]

$$I_{\text{out}} = \frac{I_{\text{in}} \eta T^2 G}{[(1 - RG)^2 + 4RG \sin^2 \varphi]}, \tag{1}$$

where η is the light coupling coefficient into active region, and $T = 1 - R$ represents the intensity transmittance of the mirror. G is defined as

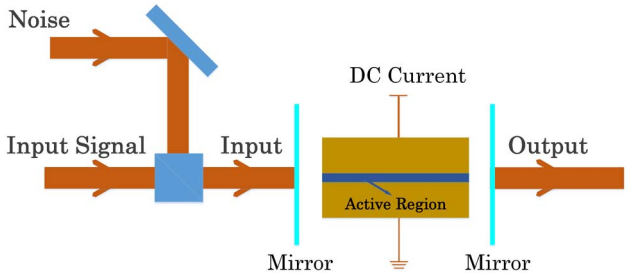

Fig. 1. Schematic diagram of the stochastic resonance system.

$$G = \exp[(g - \alpha)L], \tag{2}$$

where α is the loss coefficient, and the saturated gain coefficient g can be written as

$$g = \frac{g_0}{\left(1 + \frac{I_{\text{out}}}{I_s}\right)}, \tag{3}$$

where I_s is the saturation output intensity of amplifier, and g_0 is the small signal gain coefficient. The single-path phase shift φ across the cavity is given by

$$\varphi = \varphi_0 + \frac{\left(\frac{b}{2}\right) g_0 L}{\left(\frac{I_{\text{out}}}{I_s}\right)\left(1 - \frac{I_{\text{out}}}{I_s}\right)}, \tag{4}$$

where φ_0 is the initial phase detuning, and b, called the antiguidance factor, is the ratio of the real to imaginary index changes.

To acquire the optical bistability in the SOA, two basic mechanisms are required: feedback and nonlinearity[22]. The feedback is provided by the multiple reflections inside the F-P cavity, and the microscopic optical nonlinearity is the nonlinear response of the active layer to the refractive index.

The optical bistable hysteresis is acquired by solving Eqs. (1)–(4) in the SOA, as shown in Fig. 2. The typical parameters for the SOA are $\alpha = 20\ \text{cm}^{-1}$, $\eta = 0.75$, and $g_0 = 280\ \text{cm}^{-1}$. It can be seen that the output intensity varies non-monotonically with the input intensity and the hysteresis curve switch between the two stable states when the values of the input intensity are 0.18 and 1.72 MW/cm^2, respectively. In this case, the frequency of the input light is adopted below the F-P cavity resonance frequency. With the increase of input intensity, the refractive index of the active medium increases due to the decrease of carrier density, shifting the resonance frequency toward lower values[23]. When the resonance frequency approaches the signal frequency, the output jumps suddenly to the upper branch of the bistable loop by the runaway effect as a result of the feedback of the F-P cavity. On the contrary, the output drops to the lower branch of the hysteresis curve as the input intensity decreases.

To achieve the stochastic resonance based on optical bistability in the SOA, we analyze the influence of the

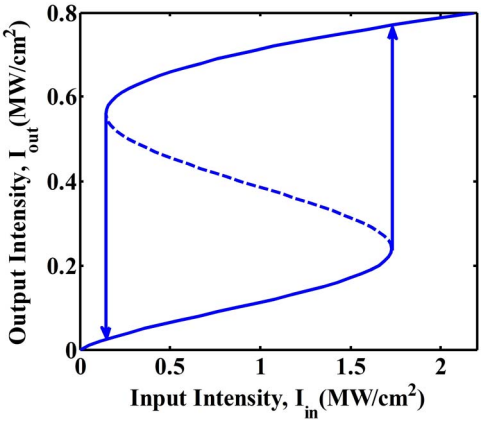

Fig. 2. Optical bistable hysteresis in the SOA with $\alpha = 20\ \text{cm}^{-1}$, $\eta = 0.75$, $g_0 = 280\ \text{cm}^{-1}$, $L = 300\ \mu\text{m}$, $b = 2$, $\varphi_0 = \frac{\pi}{4}$, and $R = 0.3$.

dominant system parameters on the bistable property. Figure 3 depicts the input-output characteristics of the SOA for various cavity lengths L and reflectivity R values, and the adopted parameters $\alpha = 20\ \text{cm}^{-1}$, $\eta = 0.75$, $g_0 = 240\ \text{cm}^{-1}$, $b = 3$, and $\varphi_0 = \frac{\pi}{4}$. It can be seen in Fig. 3(a) that the bistability generates more easily as L increases from 100 to 400 μm, but the output intensity and the width of the bistable region decreases. It is explained for the characteristics that when the cavity length L increases as the F-P resonance wavelength increases, the threshold intensity of optical bistability is reduced as a result of the resonance frequency shifting toward the frequency of the input light. Figure 3(b) shows the bistability curves for different R values with $L = 300\ \mu\text{m}$ and the same parameter values as Fig. 3(a). As illustrated in Fig. 3(b), a higher reflectivity increases the input intensity to open the optical switch duo to more input light coupling into the F-P cavity. However, when the reflection coefficient is below 0.1, the feedback is insufficient to create a bistability output for a given input intensity.

In addition to the above parameters, the roles of the initial phase detuning φ_0 and antiguidance factor b in the bistable system are investigated. Figure 4(a) illustrates the input-output characteristics of the bistable system

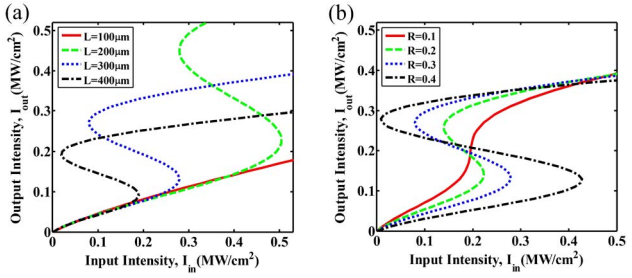

Fig. 3. Bistable output characteristics with different system parameters of the SOA: (a) $b = 3$, $\varphi_0 = \frac{\pi}{4}$, $R = 0.3$, and $L =$ 100 μm (red), 200 μm (green), 300 μm (blue), and 400 μm (black); (b) $L = 300\ \mu\text{m}$, $b = 3$, $\varphi_0 = \frac{\pi}{4}$, and $R = 0.1$ (red), 0.2 (green), 0.3 (blue), and 0.4 (black).

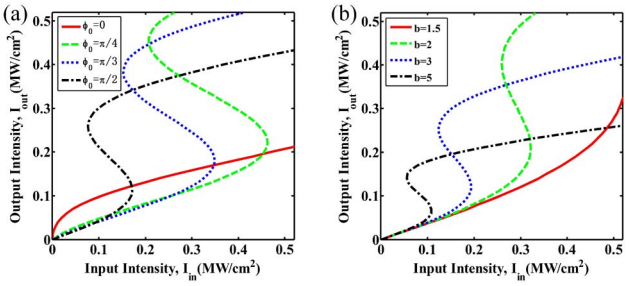

Fig. 4. Bistability characteristics with different parameters: (a) $R = 0.3$, $L = 300$ μm, $b = 3$, and $\varphi_0 = 0$ (red), $\frac{\pi}{4}$ (green), $\frac{\pi}{3}$ (blue), and $\frac{\pi}{2}$ (black); (b) $R = 0.3$, $L = 300$ μm, $\varphi_0 = \frac{\pi}{4}$, and $b =$ 1.5 (red), 2 (green), 3 (blue), and 4 (black).

for various φ_0 in the SOA with the parameters $\alpha = 20\ \mathrm{cm}^{-1}$, $\eta = 0.75$, $R = 0.3$, $g_0 = 240\ \mathrm{cm}^{-1}$, $b = 3$, and $L = 300$ μm. When the initial phase detuning is zero [the green curve in Fig. 4(a)], the system does not exhibit bistability as a result of the transmission playing a leading role. If phase detuning is introduced, a point is reached where the system is bistable. As shown in Fig. 4(b) for the different b-values with $\varphi_0 = \pi/4$ and the same parameter values as Fig. 4(a), it is clear that the steady-state bistable output can be acquired at a lower input intensity as the antiguidance factor b increases.

It is concluded from Figs. 3 and 4 that the output properties of bistability depend strongly upon the above four system parameters. The initial phase detuning and reflectivity must satisfy the following requirements: $\varphi_0 > 0$, and $R > 0.1$. Furthermore, the bistability results more easily when the values of cavity length L and antiguidance factor b become large; however, too large values of L and b lead to a small output.

The nonlinear dynamics model of the stochastic resonance is usually described by the Langevin equation[22], which is variational at different bistable systems. The Langevin equation in the SOA for output I_{out} and input I_{in} can be written as[24]

$$\frac{\mathrm{d}I_{\mathrm{out}}(t)}{\mathrm{d}t} = -\frac{\mathrm{d}V(I_{\mathrm{out}})}{\mathrm{d}I_{\mathrm{out}}}, \tag{5}$$

where $V(I_{\mathrm{out}})$ denotes the potential function of a bistable system which can be given by

$$V(I_{\mathrm{out}}) = -\int_0^{I_{\mathrm{out}}} \left[I_{\mathrm{in}} - \frac{I_{\mathrm{out}}\eta T^2 G}{(1-RG)^2 + 4RG\sin^2\varphi} \right] \mathrm{d}I_{\mathrm{out}}. \tag{6}$$

To extract signals buried in noise via stochastic resonance in the SOA, we use the schematic diagram shown in Fig. 1. A mixture of a periodic signal pulses' light and noise light are sent into a laser diode with GaAs active layer. The input light intensity can be expressed as

$$I_{\mathrm{in}}(t) = S(t) + N(t), \tag{7}$$

where $\mathrm{S}(t)$ is the input signal assumed as a Gaussian pulse with a certain peak intensity, which is given by

$$S(t) = S_0 \exp[-2(t/t_p)^2], \tag{8}$$

where S_0 is the peak intensity of signal and t_p is the pulse width, respectively. $N(t)$ is the noise with the autocorrelation function $N(t)N(0) = 2D_N\delta(t)$ and D_N is the noise intensity[25]. To apply the optical bistability to the stochastic resonance, the higher bistable output efficiency and the wider bistable region are necessary. According to the above analysis and conclusion, the fitting parameter values for simulation are adopted as $\alpha = 20\ \mathrm{cm}^{-1}$, $\eta = 0.75$, $g_0 = 240\ \mathrm{cm}^{-1}$, $L = 300$ μm, $R = 0.3$, $\varphi_0 = \pi/4$, $b = 3$, and $t_p = 7.5$ ms.

In order to investigate the stochastic resonance in the SOA, we set the signal intensity $S_0 = 0.5\ \mathrm{MW/cm}^2$ with an increasing normalized noise intensity D from 0 to 10. Here, the $D = D_N/S_0$ denotes the noise-to-signal ratio.

Figure 5 shows transmission properties of the stochastic resonance system under different input noise intensities. As shown in Figs. 5(a) and 5(a′), the initial signal is

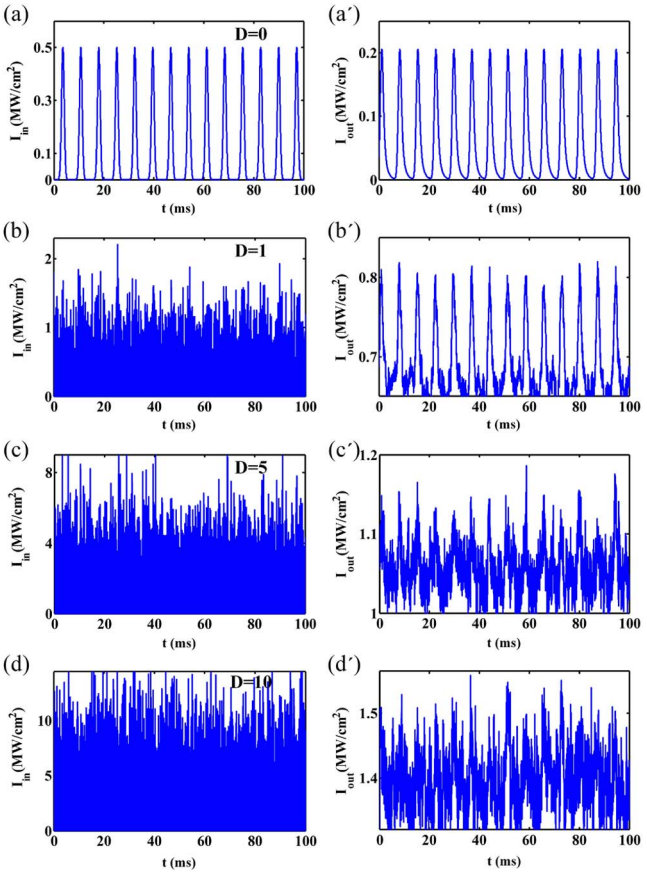

Fig. 5. Transmission properties of the stochastic resonance system with increasing noise intensities. (a)–(d) input signals $S_0 =$ 0.5 MW/cm^2 with noise, in which normalized noise intensities D are 0:1, 1:1, 5:1, and 10:1, respectively; (a′)–(d′) the corresponding output signals through the stochastic resonance system with parameters $L = 300$ μm, $R = 0.3$, $\varphi_0 = \frac{\pi}{4}$, and $b = 3$.

insufficient to overcome the bistable threshold to reach a higher output by itself. Figure 5(b) shows that the output signal is almost consistent with the input pulse signal in addition to some minor deformations at the lower edge of output intensity curve. The signal overwhelmed by noise can be extracted effectively with a high approximation. However, in Figs. 5(c′) and 5(d′), the output signals gradually become indistinguishable and distorted compared to the pure input signals when the noise intensity is further increased, as shown in Figs. 5(c) and 5(d). Consequently, Fig. 5 indicates that the signals can be effectively extracted from the noise background via the stochastic resonance system when the input signal-to-noise ratio (SNR) is set at an applicable range. If the level of the input noise is too high, the output signals relative to the pure input signals will be seriously distorted due to the leading role of the input noise.

To evaluate the ability of the stochastic resonance system to extract signals from the overwhelmed noise, the cross-correlation coefficient is used to quantitatively measure the SNR improvement by comparing the similarity between the input signals and the output signals. The cross-correlation coefficients can be expressed as[9]

$$C_{\text{in}} = \langle I_{\text{in}}(t)|S(t)\rangle, \qquad C_{\text{out}} = \langle I_{\text{out}}(t)|S(t)\rangle, \tag{9}$$

where $S(t)$ is the input signal, $I_{\text{in}}(t)$ is the input signal with the additive noise, and $I_{\text{out}}(t)$ is the output signal, respectively. Thus, the cross-correlation gain can be written as $C_g = C_{\text{out}}/C_{\text{in}}$.

In Figs. 6(a) and 6(b), we consider the cross-correlation coefficients C_{in} and C_{out} and the cross-correlation gain C_g as a function of the normalized noise intensity D for the fixed input signal intensity $S_0 = 0.5$ MW/cm^2. As the normalized noise intensity is increased from 0 to 10, the C_{in} is drastically decreased because the noise is more forceful than the signal, especially since D is smaller in the initial case, but the C_{out} relative to the C_{in} gently falls off, as shown in Fig. 6(a). The cross-correlation gain is analyzed by numerically fitting the C_g value for different levels of normalized noise intensity. As shown in Fig. 6(b), the cross-correlation gain increases to a maximum value of nine first, and then begins to drop dramatically. As the noise intensity increases, the stochastic resonance system becomes increasingly dominated by the noise, which leads to the distortion of the extracted signals. Too little noise disables the reversal of the threshold, but too much noise leads to an excessive distortion. Therefore, there exists an optimal noise level for acquiring the maximum cross-correlation gain, which is the signature of the stochastic resonance.

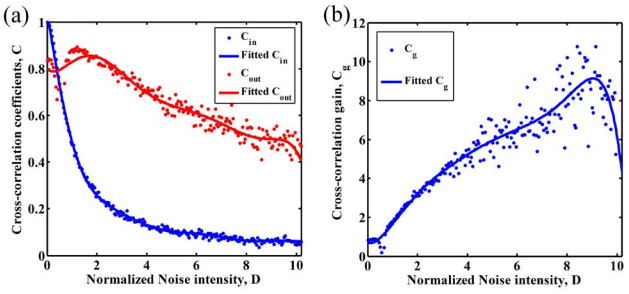

Fig. 6. (a) Cross-correlation coefficients and (b) the cross-correlation gain as functions of the normalized noise intensity D at system parameters $L = 300$ μm, $R = 0.3$, $\varphi_0 = \frac{\pi}{4}$, and $b = 3$. The solid curves are the optimal fitted curves neglecting the random fluctuation.

In conclusion, we report a novel scheme of extracting pulse signals buried in noise via stochastic resonance in the SOA. The formation mechanism and the impact factors of the optical bistable loop are analyzed at different cavity lengths, mirror reflectivity, initial phase detuning, and antiguidance factors. Based on the stochastic differential equation of the bistable system with a periodic pulse signal, we demonstrate the transmission features and the cross-correlation gain in the case of additive noise actions. It is confirmed that the appropriate noise level and dynamic hysteresis enhance the stochastic resonance effect of the SOA. The result shows that the stochastic resonance in the SOA has potential applications for weak signal extraction in all-optical signal processing.

This work was supported by the National Natural Science Foundation of China under Grant No. 61275134.

References

1. R. Benzi, A. Sutera, and A. Vulpiani, J. Phys. A Math. Gen. **14**, L453 (1981).
2. J. M. Vilar, A. Pérezmadrid, and J. M. Rubí, Phys. Rev. E Stat. Phys. Plasmas Fluids Relat. Interdiscip. Top. **54**, 6929 (1996).
3. J. K. Douglass, L. Wilkens, E. Pantazelou, and F. Moss, Nature **365**, 337 (1993).
4. D. S. Leonard and L. E. Reichl, Phys. Rev. E Stat. Phys. Plasmas Fluids Relat. Interdiscip. Top. **49**, 1734 (1994).
5. S. Fauve and F. Heslot, Phys. Lett. A **97**, 5 (1983).
6. J. J. Collins, T. T. Imhoff, and P. Grigg, J. Neurophysiol. **76**, 642 (1996).
7. W. C. Stacey and D. M. Durand, J. Neurophysiol. **83**, 1394 (2000).
8. Y. Yu, W. Wang, J. Wang, and F. Liu, Phys. Rev. E Stat. Nonlinear Soft Matter Phys. **63**, 142 (2001).
9. D. V. Dylov, J. W. Fleischer, D. V. Dylov, and J. W. Fleischer, Nat. Photon. **4**, 323 (2010).
10. Q. Sun, H. Liu, H. Nan, Z. Wang, H. Jing, and S. Li, Sci. Rep. **5**, 16183 (2015).
11. H. Jing, L. Hongjun, S. Qibing, H. Nan, W. Zhaolu, and L. Shaopeng, Opt. Lett. **40**, 5367 (2015).
12. M. I. Dykman, A. L. Velikovich, G. P. Golubev, D. G. Luchinskiĭ, and S. V. Tsuprikov, Zhetf Pisma Redaktsiiu **53**, 182 (1991).
13. M. Francesco, G. Massimo, B. Stéphane, and B. Salvador, Phys. Rev. Lett. **88**, 131 (2002).
14. K. Otsuka and S. Kobayashi, Electron. Lett. **19**, 262 (1983).
15. M. J. Adams, Optoelectron. IEE Proc. J. **132**, 343 (1985).
16. A. Kannan, "Dual Signal Optical Bistability in a Semiconductor Optical Amplifier," Master Dissertations (Rochester Institute of Technology, 2015).
17. J. Qin, H. Wang, D. Wang, M. Zhang, Y. Ji, and G. Lv, Chin. Opt. Lett. **12**, 110601 (2014).

18. M. I. Dykman, G. P. Golubev, I. K. Kaufman, D. G. Luchinsky, P. V. E. Mcclintock, and E. A. Zhukov, IL Nuovo Cimento D **17**, 743 (1995).
19. H. M. Gibbs, S. S. Tarng, J. L. Jewell, D. A. Weinberger, K. Tai, A. C. Gossard, S. L. Mccall, A. Passner, and W. Wiegmann, Appl. Phys. Lett. **41**, 221 (1982).
20. L. Yu, Y. Li, J. Zang, D. Lu, B. Pan, and L. Zhao, Chin. Opt. Lett. **12**, 081402 (2014).
21. K. Otsuka and H. Iwamura, Phys. Rev. A **28**, 3153 (1983).
22. L. Gammaitoni, P. Hänggi, P. Jung, and F. Marchesoni, Rev. Modern Phys. **70**, 223 (1998).
23. J. Qin, Z. Ji, H. Wang, D. Wang, M. Zhang, and G. Lv, Chin. Opt. Lett. **10**, 010601 (2015).
24. R. Bartussek, P. Jung, and P. Hänggi, Phys. Rev. E Stat. Phys. Plasmas Fluids Relat. Interdiscip. Top. **49**, 3930 (1994).
25. L. Gammaitoni, F. Marchesoni, E. Menichella-Saetta, and S. Santucci, Phys. Rev. Lett. **65**, 2607 (1990).